Tuning the Luminescence and Electroluminescence of Diphenylboron Complexes of 5-Substituted 2-(2′-Pyridyl)indoles

Qinde Liu,[†] Maria S. Mudadu,[‡] Hartmut Schmider,[†] Randolph Thummel,*[,‡] Ye Tao,[§] and Suning Wang*[,†]

Department of Chemistry, Queen's University, Kingston, Ontario, K7L 3N6, Canada, Department of Chemistry, University of Houston, Houston, Texas 77204-5003, and Institute for Microstructural Sciences, National Research Council, 100 Sussex Drive, Ottawa, K1A 0R6, Canada

Received June 4, 2002

To examine the effect of substituent groups on the luminescence of BPh_2(X-2-PI) complexes, three new air-stable boron complexes BPh_2(F-2-PI) (**5a**), BPh_2(Cl-2-PI) (**5b**), and BPh_2(CH_3O-2-PI) (**5c**) were synthesized and characterized, where F-2-PI = 5-fluoro-2-(2′-pyridyl)indole, Cl-2-PI = 5-chloro-2-(2′-pyridyl)indole, and CH_3O-2-PI = 5-methoxyl-2-(2′-pyridyl)indole. In these complexes, the 5-substituted 2-PI ligand chelates in a tretrahedral fashion to the boron center. Compounds **5a**−**c** are luminescent, with **5a** having the highest emission efficiency. Compared with the emission maximum of BPh_2(2-PI) (516 nm), the emission maximum of **5a** and **5b** is blue-shifted to 490 and 487 nm, respectively, while the emission of **5c** is red-shifted to 532 nm, indicating the possibility of tuning the luminescence of these complexes by varying the substituent groups on the 2-PI ligand. An electroluminescent device using compound **5a** as the emitter and the electron transport material has been fabricated.

Introduction

Luminescent organic/organometallic compounds have attracted much attention recently due to their potential applications in electroluminescent displays.[1−4] Luminescent chelate complexes have been shown to be particularly useful in electroluminescent (EL) displays because of their relatively high stability and volatility.[2,3] Although blue luminescent materials are one of the key color components necessary for full-color displays, they are still scarce. Recently, we reported two blue/green luminescent boron compounds,[5] BPh_2(2-PI) (2-PI = 2-(2′-pyridyl)indole) and BPh_2(2-PazI) (2-PazI = 2-(2′-pyridyl)-7-azaindole). It was found that although the

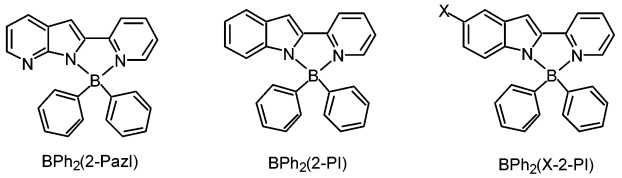

molecular structures of these two compounds are almost identical, compared with that of BPh_2(2-PI) (λ_{max} = 516 nm), the emission of BPh_2(2-PazI) is ∼40 nm blue-shifted (λ_{max} = 476 nm). The reason for this shift is that replacement of an indole CH by the more electronegative N atom lowers the HOMO level, increasing the HOMO−LUMO gap, leading to a blue shift of the emission energy. Earlier molecular orbital calculations indicated that the HOMO level of BPh_2(2-PI) consists almost entirely of atomic orbitals from the indole ring.[5] Hence, a substituent on the indole ring could have a significant impact on the luminescence of the corresponding boron complex. With the appropriate choice of a substituent group X, it may be possible to drive the emission energy of the boron complex more to the blue region.

[†] Queen's University.
[‡] University of Houston.
[§] Institute for Microstructural Sciences.

(1) (a) Tang, C. W.; VanSlyke, S. A. *Appl. Phys. Lett.* **1987**, *51*, 913. (b) Tang, C. W.; VanSlyke, S. A.; Chen, C. H. *J. Appl. Phys.* **1989**, *65*, 3611. (c) Shirota, Y.; Kawami, S.; Imai, K. *Appl. Phys. Lett.* **1994**, *65*, 807. (d) Hamada, Y.; Sana, T.; Fujita, M.; Fujii, T.; Nishio, Y.; Shibata, K. *Jpn. J. Appl. Phys.* **1993**, *32*, L514. (e) Bulovic, V.; Gu. G.; Burrows, P. E.; Forrest, S. R. *Nature* **1996**, *380*, 29. (f) Braun, M.; Gmeiner, J.; Tzolov, M.; Coelle, M.; Meyer, F. D.; Milius, W.; Hillebrecht, H.; Wendland, O.; von Schutz, J. U.; Brutting, W. *J. Chem. Phys.* **2001**, *114*, 9625. (g) Schmidaur, H.; Lettenbauer, J.; Wikinson, D. L.; Müller, G.; Kumberger, O. *Z. Naturforsch.* **1991**, *46b*, 901.

(2) (a) Shen, Z.; Burrows, P. E.; Bulovic, V.; Borrest, S. R.; Thompson, M. E. *Science* **1997**, *276*, 2009. (b) Baldo, M. A.; Lamansky, S.; Burrows, P.; Thompson, M. E.; Forrest, S. R. *Appl. Phys. Lett.* **1999**, *75*, 5. (c) Kwong, R. C.; Sibley, S.; Dubovoy, T.; Baldo, M.; Forrest, S. R.; Thompson, M. E. *Chem. Mater.* **1999**, *11*, 3709 (d) Adachi, C.; Baldo, M. A.; Forrest, S. R.; Thompson, M. E. *Appl. Phys. Lett.* **2000**, *77*, 904. (e) Lamansky, S.; Djurovich, P.; Murphy, D.; Abdel-Razzaq, F.; Lee, H. E.; Adachi, C.; Burrows, P. E.; Forrest, S. R.; Thompson, M. E. *J. Am. Chem. Soc.* **2001**, *123*, 4304.

(3) (a) Li, Y.; Liu, Y.; Bu, W.; Guo, J.; Wang, Y. *Chem. Commun.* **2000**, 1551. (b) Popovic, Z. D.; Aziz, H.; Hu, N.-X.; Ioannidis, A.; dos Anjos, P. N. M. *J. Appl. Phys.* **2001**, *89*, 4673. (c) Adachi, C.; Tokito, S.; Tsutsui, T.; Saito, S. Jpn. *J. Appl. Phys.* **1988**, *27*, L713. (d) Adachi, C.; Tsutsui, T.; Saito, S. *Appl. Phys. Lett.* **1990**, *56*, 799. (e) Tao, X. T.; Suzuki, H.; Wada, T.; Sasabe, H.; Miyata, S. *Appl. Phys. Lett.* **1999**, *75*, 1655. (f) Aziz, H.; Popovic, Z. D.; Hu, N.-X.; Hor, A.-M.; Xu, G. *Science* **1999**, *283*, 1900.

(4) (a) Hu, N.-X.; Esteghamatian, M.; Xie, S.; Popovic, P.; Ong, B.; Hor, A.-M.; Wang, S. *Adv. Mater.* **1999**, *11*, 1460. (b) Hamada, Y.; Sana, T.; Fujii, T.; Nishio, Y.; Takahashi, H.; Shibata, K. *Appl. Phys. Lett.* **1997**, *71*, 3338. (c) Hamada, Y.; Sano, T.; Fujita, M.; Fujii, T.; Nishio, Y.; Shibata, K. *Chem. Lett.* **1993**, 905. (d) Wu. Q.; Esteghamatian, M.; Hu, N.-X.; Popovic, Z.; Enright, G.; Tao, Y.; D'Iorio, M.; Wang, S. *Chem. Mater.* **2000**, *12*, 79.

(5) Liu, S.-F.; Wu, Q.; Schmider, H. L.; Aziz, H.; Hu, N.-X.; Popovic, Z.; Wang, S. *J. Am. Chem. Soc.* **2000**, *122*, 3671.

10.1021/om020446j CCC: $22.00
Publication on Web 10/01/2002

As part of our continuing search for stable blue emitters, we have examined the effect of three different substituents in the 5-position of indole on the luminescence of their diphenylboron complexes BPh_2(X-2-PI). Two ligands containing electron-withdrawing fluoro and chloro groups, 5-fluoro-2-(2′-pyridyl)indole (F-2-PI) and 5-chloro-2-(2′-pyridyl)indole (Cl-2-PI), and one ligand containing an electron-donating methoxy group, 5-methoxy-2-(2′-pyridyl)indole (CH_3O-2-PI), were synthesized, and the corresponding boron compounds were prepared. The details of the syntheses, structures, and luminescent and electroluminescent properties of the boron complexes are reported.

Experimental Section

All starting materials were purchased from Aldrich Chemical Co. except triphenylboron, which was purchased from Strem Chemical Co. ^{1}H NMR spectra were recorded on a Bruker Advance spectrometer at 300 MHz for ^{1}H and 75 MHz for ^{13}C. Elemental analyses of C, H, and N were performed by Canadian Microanalytical Service, Ltd, Delta, British Columbia, and QTI, Rt 22 East, Whitehouse, NJ. Excitation and emission spectra were obtained with a Photon Technologies International QuantaMaster Model 2 spectrometer. UV−vis spectra were recorded on a Hewlett-Packard 8562A diode array spectrophotometer. The syntheses of boron compounds were carried out under a nitrogen atmosphere.

4′-Fluorophenylhydrazone of 2-Acetylpyridine (3a). A mixture of 2-acetylpyridine (0.61 g, 5.0 mmol), 4-fluorophenylhydrazine hydrochloride (0.97 g, 6.0 mmol), and glacial AcOH (2 drops) in absolute EtOH (10 mL) was refluxed for 3 h. After cooling to room temperature, the precipitate was filtered to provide **3a** as an orange solid (1.12 g, 97%); mp 252−254 °C. ^{1}H NMR (DMSO-d_6, δ, ppm): 10.43 (s, 1H), 8.70 (d, 1H, J = 5.7 Hz), 8.40 (t, 1H, J = 7.5 Hz), 8.23 (d, 1H, J = 8.1 Hz), 7.74 (t, 1H, J = 6.0 Hz), 7.59−7.63 (m, 2H), 7.14 (td, 2H, J = 9.0, 0.6 Hz), 2.39 (s, 3H).

4′-Chlorophenylhydrazone of 2-Acetylpyridine (3b). In the manner described for **3a**, a mixture of 2-acetylpyridine (0.61 g, 5.0 mol), 4-chlorophenylhydrazine hydrochloride (1.18 g, 6.0 mmol), and glacial AcOH (2 drops) in absolute EtOH (8 mL) provided **3b** as an orange solid (1.16 g, 95%); mp 243−246 °C. ^{1}H NMR (DMSO-d_6, δ, ppm): 10.39 (s, 1H), 8.72 (d, 1H, J = 5.4 Hz), 8.37 (t, 1H, J = 7.5 Hz), 8.25 (d, 1H, J = 8.4 Hz), 7.74 (t, 1H, J = 6.9 Hz), 7.57 (d, 2H, J = 9.0 Hz), 7.36 (d, 2H, J = 8.7 Hz), 2.40 (s, 3H).

4′-Methoxyphenylhydrazone of 2-Acetylpyridine (3c). In the manner described for **3a**, a mixture of 2-acetylpyridine (0.97 g, 8.0 mol), 4-methoxyphenylhydrazine hydrochloride (1.68 g, 9.6 mmol), and glacial AcOH (2 drops) in absolute EtOH (11 mL) provided **3c** as an orange solid (1.76 g, 91%); mp 218−220 °C. ^{1}H NMR (DMSO-d_6, δ, ppm): 10.34 (s, 1H), 8.67 (d, 1H, J = 5.4 Hz), 8.41 (t, 1H, J = 7.8 Hz), 8.21 (d, 1H, J = 8.4 Hz), 7.73 (t, 1H, J = 6.3 Hz), 7.57 (d, 2H, J = 7.5 Hz), 6.89 (d, 2H, J = 8.7 Hz), 3.73 (s, 3H), 2.37 (s, 3H).

5-Fluoro-2-(2′-pyridyl)indole (4a). A mixture of **3a** (0.61 g, 2.6 mmol) and polyphophoric acid (PPA, 4.13 g) was mechanically stirred at 120 °C for 3 h. After cooling to room temperature, 10% NaOH was added until pH 14 was obtained. The mixture was extracted with CH_2Cl_2 (3 × 30 mL), and the combined organic phase was washed with brine (20 mL), dried ($MgSO_4$), and concentrated. Chromatography on silica gel, eluting with EtOAc, followed by sublimation (115−120 °C, 0.5 mmHg) provided **4a** (0.22 g, 39%) as a white solid; mp 147−148 °C. ^{1}H NMR (DMSO-d_6, δ, ppm): 9.76 (s, 1H), 7.78 (dd, 1H, J = 4.8, 0.9 Hz), 7.78 (d, 1H, J = 7.5 Hz), 7.73 (t, 1H, J = 7.2 Hz), 7.25−7.31 (m, 2H), 7.19 (t, 1H, J = 6.0 Hz), 6.92−6.99 (m, 2H). ^{13}C NMR ($CDCl_3$, δ, ppm): 158.3 (d, J_{C-F} = 233.2 Hz, indolyl), 150.4 (py), 149.3 (indolyl), 138.6 (py), 137.0 (py), 133.5 (indolyl), 129.5 (d, J_{C-F} = 10.3 Hz, indolyl), 122.5 (py), 120.3 (py), 112.2 (d, J_{C-F} = 9.7 Hz, indolyl), 112.1 (d, J_{C-F} = 26.3 Hz, indolyl), 105.8 (d, J_{C-F} = 23.2 Hz, indolyl), 100.8 (d, J_{C-F} = 4.9 Hz, indolyl). Anal. Calcd for $C_{13}H_{19}FN_2$: C, 73.58; H, 4.25; N, 13.21. Found: C, 73.30; H, 3.98; N, 13.03.

5-Chloro-2-(2′-pyridyl)indole (4b). In the manner described for **4a**, a mixture of **3b** (1.86 g, 7.6 mmol) and PPA (12.00 g) provided **4b** as a white solid, which was recrystallized from absolute EtOH (1.14 g, 65%); mp 173−175 °C. ^{1}H NMR (DMSO-d_6, δ, ppm): 11.86 (s, 1H), 8.63 (dd, 1H, J = 4.8, 0.9 Hz), 8.00 (dd, 1H, J = 8.1, 0.9 Hz), 7.88 (td, 1H, J = 7.5, 1.8 Hz), 7.62 (d, 1H, J = 2.1 Hz), 7.48 (d, 1H, J = 8.1 Hz), 7.34 (ddd, 1H, J = 8.7, 4.8, 1.5 Hz), 7.13 (s, 1H), 7.11 (dd, 1H, J = 8.7, 2.1 Hz). ^{13}C NMR ($CDCl_3$, δ, ppm): 150.1 (py), 149.3 (indolyl), 138.2 (py), 137.0 (py), 135.1 (indolyl), 130.3 (indolyl), 126.0 (indolyl), 123.7 (py), 122.6 (py), 120.6 (indolyl), 120.2 (indolyl), 112.6 (indolyl), 100.3 (indolyl). Anal. Calcd for $C_{13}H_{19}ClN_2$: C, 68.42; H, 3.95; N, 12.28. Found: C, 68.07; H, 3.78; N, 12.17.

5-Methoxyl-2-(2′-pyridyl)indole (4c). A solution of **3c** (0.70 g, 2.9 mmol) in glacial HOAc (10 mL) was refluxed under Ar for 28 h. After cooling to room temperature, 10% NaOH was added until pH 14 was obtained. The mixture was extracted with CH_2Cl_2 (3 × 50 mL), and the combined organic phase was washed with brine (20 mL), dried ($MgSO_4$), and concentrated. Chromatography on silica gel eluting with CH_3Cl/EtOAc (4:1) provided **4c**, which was recrystallized from benzene/hexane (0.17 g, 11%); mp 128−129 °C. ^{1}H NMR (DMSO-d_6, δ, ppm): 11.53 (s, 1H), 8.60 (d, 1H, J = 4.8 Hz), 7.95 (d, 1H, J = 8.1 Hz), 7.84 (td, 1H, J = 7.5, 1.8 Hz), 7.34 (d, 1H, J = 8.7 Hz), 7.27 (dd, 1H, J = 7.2, 5.1 Hz), 7.05 (s, 2H), 6.77 (dd, 1H, J = 8.7, 2.1 Hz), 3.76 (s, 1H). ^{13}C NMR ($CDCl_3$, δ, ppm): 154.5 (indolyl), 150.7 (py), 149.1 (indolyl), 137.5 (py), 136.8 (py), 132.4 (indolyl), 129.6 (indolyl), 122.0 (py), 120.0 (py), 114.0 (indolyl), 112.3 (indolyl), 102.6 (indolyl), 100.7 (indolyl), 55.9 (methyl). Anal. Calcd for $C_{13}H_{19}N_2O$: C, 75.00; H, 5.36; N, 12.50. Found: C, 74.87; H, 5.27; N, 12.34.

BPh_2(F-2-PI) (5a). A mixture of **4a** (50 mg, 0.24 mmol) and triphenylboron (57 mg, 0.24 mmol) was dissolved in dry toluene (pretreated with P_2O_5 and freshly distilled). The solution was refluxed for 6 h under nitrogen. After removing the solvent under vacuum, the residue was dissolved in THF/toluene (1:3) and the solution was allowed to stand at room temperature under nitrogen. Slow evaporation of solvent gave yellowish green crystals of **5a** after 2 weeks (52 mg, 58%), mp 290−292 °C. ^{1}H NMR (CD_2Cl_2, δ, ppm): 8.46 (dt, 1H, J = 5.8, 1.1 Hz), 8.10 (ddd, 1H, J = 8.1, 7.3, 1.4 Hz), 8.02 (dt, 1H, J = 8.1, 1.1 Hz), 7.38 (m, 3H), 7.27 (m, 9H), 7.19 (tt, 1H, J = 4.7, 0.5 Hz), 7.16 (s, 1H), 6.87 (td, 1H, J = 9.0, 2.6 Hz). ^{13}C NMR (CD_2Cl_2, δ, ppm): 158.6 (J_{C-F} = 234.2 Hz, indolyl), 149.8 (indolyl), 143.2 (py), 142.2 (py), 138.9 (ph), 136.4 (indolyl), 133.8 (ph), 133.3 (J_{C-F} = 10.5 Hz, indolyl), 128.3 (ph), 127.6 (ph), 122.7 (py), 119.7 (py), 115.1 (J_{C-F} = 9.8 Hz, indolyl), 112.7 (J_{C-F} = 26.8 Hz, indolyl), 106.7 (J_{C-F} = 23.2, indolyl), 99.0 (J_{C-F} = 5.8 Hz, indolyl) (one quaternary carbon hidden). Anal. Calcd for $C_{25}H_{18}BFN_2$: C, 79.83; H, 4.79; N, 7.45. Found: C, 79.72; H, 4.79; N, 7.44.

BPh_2(Cl-2-PI) (5b). In the manner described for **5a**, a mixture of **4b** (50 mg, 0.21 mmol) and triphenylboron (47 mg, 0.21 mmol) provided **5b** as yellowish green crystals (41 mg, 50%), mp 297−298 °C. ^{1}H NMR (CD_2Cl_2, δ, ppm): 8.47 (dt, 1H, J = 5.9, 1.2 Hz), 8.10 (ddd, 1H, J = 8.2, 7.3, 1.4 Hz), 8.02 (dt, 1H, J = 8.1, 1.2 Hz), 7.72 (dd, 1H, J = 2.0, 0.4 Hz), 7.39 (ddd, 1H, J = 7.3, 5.9, 1.4 Hz), 7.27 (m, 10H), 7.19(dt, 1H, J = 8.8, 0.7 Hz), 7.14 (d, 1H, J = 0.8 Hz), 7.05 (dd, 1H, J = 8.8, 2.1 Hz). ^{13}C NMR (CD_2Cl_2, δ, ppm): 149.4 (indolyl), 143.0 (py), 142.0 (py), 138.4 (ph), 137.6 (indolyl), 134.0 (indolyl), 133.5 (ph), 128.1 (ph), 127.4 (ph), 125.6 (indolyl), 123.8 (py), 122.6 (py), 121.6 (indolyl), 119.5 (indolyl), 115.1 (indolyl), 98.3 (indolyl) (one quaternary carbon hidden). Anal. Calcd for

Table 1. Data Collection and Processing Parameters for 5a−c

	5a	5b	5c
formula	$C_{25}H_{18}BFN_2$	$C_{25}H_{18}BClN_2$	$C_{26}H_{21}BN_2O$
fw	376.22	392.67	388.26
space group	*C*2/*c*	*C*2/*c*	$P\bar{1}$
a/Å	18.486(3)	18.383(5)	7.2396(14)
b/Å	11.5197(18)	11.632(3)	11.480(2)
c/Å	18.403(3)	18.799(5)	12.598(3)
α/deg	90	90	84.200(4)
β/deg	95.083(3)	98.814(5)	76.205(4)
γ/deg	90	90	78.795(4)
V/Å^3	3903.8(11)	3972.3(18)	995.9(3)
Z	8	8	2
D_c/g cm^{-3}	1.280	1.313	1.295
μ/cm^{-1}	0.81	2.06	0.78
$2\theta_{max}$/deg	56.6	56.6	56.6
no. of reflns measd	13878	14066	7226
no. of reflns used (R_{int})	4663 (0.0160)	4776 (0.0542)	4554 (0.0257)
no. of variables	334	334	343
final *R* [$I > 2\sigma(I)$]			
R1[a]	0.0376	0.0523	0.0469
wR2[b]	0.1002	0.1112	0.0658
R (all data)			
R1	0.0609	0.1370	0.1439
wR2	0.1100	0.1336	0.0792
goodness of fit on F^2	1.010	0.813	0.744

$C_{25}H_{18}BClN_2$: C, 76.48; H, 4.59; N, 7.14. Found: C, 76.32; H, 4.64; N, 7.03.

BPh_2(CH$_3$O-2-PI) (5c). In the same manner as described for **5a**, a mixture of **4c** (50 mg, 0.22 mmol) and triphenylboron (54 mg, 0.22 mmol) provided **5c** as yellow crystals (42 mg, 49%), mp 251−253 °C. ^{1}H NMR (CD_2Cl_2, δ, ppm): 8.42 (dt, 1H, J = 5.9, 1.0 Hz), 8.08 (ddd, 1H, J = 8.2, 7.3, 1.4 Hz), 7.97 (dt, 1H, J = 8.1, 1.1 Hz), 7.32 (ddd, 1H, J = 7.2, 5.9, 1.3 Hz), 7.26 (m, 10H), 7.16 (d, 1H, J = 2.4 Hz), 7.13 (dd, 1H, J = 9.0, 0.5 Hz), 7.10 (d, 1H, J = 0.7 Hz), 6.77 (dd, 1H, J = 8.9, 2.5 Hz), 3.85 (s, 3H). ^{13}C NMR (CD_2Cl_2, δ, ppm): 154.9 (indolyl), 150.1 (indolyl), 143.1 (py), 142.0 (py), 137.7 (ph), 135.4 (indolyl), 133.8 (ph), 133.7 (indolyl), 128.3 (ph), 127.5 (ph), 122.0 (py), 119.3 (py), 115.4 (indolyl), 115.1 (indolyl), 103.0 (indolyl), 98.6 (indolyl), 56.2 (methyl) (one quaternary carbon hidden). Anal. Calcd for $C_{26}H_{21}BN_2O$: C, 80.45; H, 5.42; N, 7.22. Found: C, 80.28; H, 5.47; N, 7.22.

X-ray Crystallographic Analysis. Crystals were obtained from THF/toluene solutions and were mounted on glass fibers. Data were collected on a Siemens P4 single-crystal X-ray diffractometer with a CCD-1000 detector and graphite-monochromated Mo Kα radiation, operating at 50 kV and 30 mA at 25 °C. The data collection ranges over the 2θ range are 4.18−56.6° for **5a**, 4.38−56.6° for **5b**, and 3.34−56.7° for **5c**. No significant decay was observed for all samples. Data were processed on a PC using the Bruker SHELXTL software package[6] (version 5.10) and are corrected for Lorentz and polarization effects. The crystal structures of **5a**,**b** are isomorphous and belong to the monoclinic space group *C*2/*c*. The crystals of **5c** belong to triclinic space group $P\bar{1}$. All structures were solved by direct methods. All non-hydrogen atoms were refined anisotropically. All aromatic hydrogen atoms were located directly from difference Fourier maps. The hydrogen atoms of the methyl group in **5c** were calculated, and their contribution were included. The crystallographic data for compounds **5a**−**c** are given in Table 1. Selected bond lengths and angles for **5a**−**c** are listed in Table 2.

Fabrication of Electroluminescent Devices. The EL device using **5a** as the emitting layer and the electron transport layer was fabricated on an indium−tin oxide (ITO) substrate. Organic layers and the metal cathode layer were deposited on the substrate by conventional vapor vacuum deposition. Prior to the deposition, all organic materials were purified via a train sublimation method.[7] *N*,*N*′-Di-1-naphthyl-*N*,*N*′-diphenylbenzidine (NPB) was employed as the hole transport layer in the device. The device stucture can be expressed as ITO/NPB(50 nm)/BPh_2(F-2-PI)(50 nm)/Al(150 nm)/Ag(80 nm).

Table 2. Selected Bond Lengths (Å) and Angles (deg) for 5a−c and BPh_2(2-py-in)$_2$

	Complex **5a**		
B(1)−N(2)	1.5538(15)	N(2)−B(1)−C(1)	112.91(9)
B(1)−C(1)	1.6072(16)	N(2)−B(1)−C(7)	111.51(9)
B(1)−C(7)	1.6165(17)	C(1)−B(1)−C(7)	117.76(10)
B(1)−N(1)	1.6326(16)	N(2)−B(1)−N(1)	94.34(8)
C(24)−F(1)	1.3686(14)	C(1)−B(1)−N(1)	109.09(9)
		C(7)−B(1)−N(1)	108.58(9)
	Complex **5b**		
B(1)−N(2)	1.551(3)	N(2)−B(1)−C(1)	112.69(19)
B(1)−C(1)	1.596(4)	N(2)−B(1)−C(7)	112.2(2)
B(1)−C(7)	1.598(4)	C(1)−B(1)−C(7)	117.7(2)
B(1)−N(1)	1.636(3)	N(2)−B(1)−N(1)	93.93(17)
C(24)−Cl(1)	1.744(2)	C(1)−B(1)−N(1)	108.50(19)
		C(7)−B(1)−N(1)	109.06(19)
	BPh_2(2-py-in)$_2$		
B(1)−N(2)	1.561(9)	N(2)−B(1)−C(1)	111.2(6)
B(1)−C(1)	1.602(10)	N(2)−B(1)−C(7)	115.1(6)
B(1)−C(7)	1.587(10)	C(1)−B(1)−C(7)	115.4(7)
B(1)−N(1)	1.633(9)	N(2)−B(1)−N(1)	93.5(6)
		C(1)−B(1)−N(1)	110.3(6)
		C(7)−B(1)−N(1)	109.1(6)
	Complex **5c**		
B(1)−N(2)	1.568(2)	N(2)−B(1)−C(1)	113.23(16)
B(1)−C(1)	1.602(3)	N(2)−B(1)−C(7)	113.17(16)
B(1)−C(7)	1.615(3)	C(1)−B(1)−C(7)	114.99(17)
B(1)−N(1)	1.639(3)	N(2)−B(1)−N(1)	94.22(14)
C(24)−O(1)	1.408(2)	C(1)−B(1)−N(1)	110.28(16)
		C(7)−B(1)−N(1)	108.92(15)

Quantum Yield Measurements. Quantum yields of the complexes were determined relative to 9,10-diphenylanthracene in CH_2Cl_2 at 298 K (Φ_r = 0.95).[8] The absorbances of all the samples and the standard at the excitation wavelength were approximately 0.088−0.108. The quantum yields were calculated using previously known procedures.[9] The excitation wavelength is 376 nm for compounds **5a**,**b** and BPh_2(2-PI) and 396 nm for compound **5c**. The emission of the standard was measured with both 376 and 396 nm excitation, showing aborbances of 0.106 and 0.0933, respectively.

Results and Discussion

Syntheses and Structures. The 2-PI derivatives **4a**−**c** were prepared by the two-step Fischer synthesis according to a modified procedure reported previously.[10] Treatment of 2-acetylpyridine (**1**) and the appropriate phenylhydrazines **2a**−**c** afforded the corresponding phenylhydrazones **3a**−**c** in nearly quantitative yields. Polyphosphoric acid (PPA) is often an excellent acidic medium for the subsequent Fischer cyclization. The reaction of **3a**,**b** in PPA at 100−120 °C furnishes the corresponding PI derivatives **4a**,**b** in 39 and 65% yield, respectively. However, the cyclization of **3c** in PPA

(6) *SHELXTL NT*, Crystal Structure Analysis Package, Version 5.10; Bruker Axs, Analytical X-ray System: Madison, WI, 1999.

(7) Wagner, H. J.; Loutfy, R. O.; Hsiao, C. K. *J. Mater. Sci.* **1982**, *17*, 2781.

(8) Murov, S. L.; Carmichael, I.; Hug, G. L. *Handbook of Photochemistry*, 2nd ed.; Marcel Dekker: New York, 1993.

(9) Demas, N. J.; Crosby, G. A. *J. Am. Chem. Soc.* **1970**, *92*, 7262.

(10) (a) Wu, F.; Chamchoumis, C. M.; Thummel, R. P. *Inorg. Chem.* **2000**, *39*, 584. (b) Wu, F.; Hardesty, J.; Thummel, R. P. *J. Org. Chem.* **1998**, *63*, 4055. (c) Thummel, R. P.; Hegde, V. *J. Org. Chem.* **1989**, *54*, 1720.

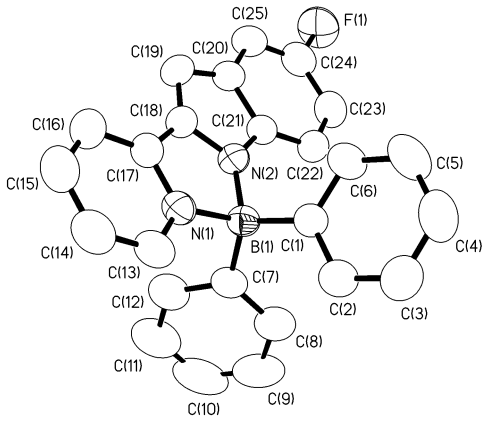

Figure 1. Molecular structure of **5a** with 50% thermal ellipsoids and labeling schemes.

Scheme 1

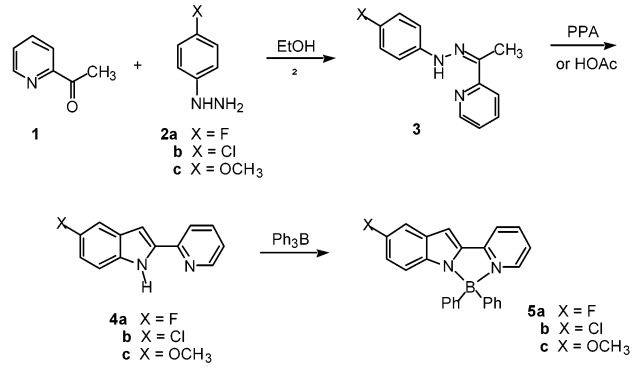

at 90−100 °C affords a complex mixture of products. Alternatively **3c** may be cyclized under milder conditions (refluxing HOAc for 18 h) to provide **4c** in 11% yield along with unreacted **3c** and its hydrolysis products.

The different cyclization behavior of the phenylhydrazones **3a**−**c** can be explained by considering the mechanism of the Fischer reaction. The key step is a [3,3]-sigmatropic rearrangement which is polarized in such a way that the intermediate diene is stabilized by an electron-withdrawing group in the phenyl ring. Therefore, the intermediate involved in the reaction of the methoxy-substituted **4c** is comparatively destabilized and thus more reactive.

The three boron complexes **5a**−**c** were all obtained in good yield by the reaction in a 1:1 ratio of triphenylboron with the corresponding ligand in toluene. Single crystals were obtained by recrystallization of the complexes from THF/toluene (1:3). Complexes **5a**−**c** were characterized by ^{1}H and ^{13}C NMR, elemental analysis, and single-crystal X-ray diffraction. All the complexes are air-stable both in the solid state and in solution. An important and common feature of **5a**−**c** is their high melting points. The melting points for **5a** and **5b** are similar, in the range 290−300 °C, about 40 °C higher than that of **5c** and the parent complex BPh_2(2-PI).

Single-crystal X-ray diffraction revealed that compounds **5a** and **5b** are isomorphous. The structure of compound **5a** is shown in Figure 1. The boron atom in **5a** has a typical tetrahedral geometry. The F-2-PI ligand is bidentately chelated to the boron center via its pyridine and indole nitrogens. The other two boron sites

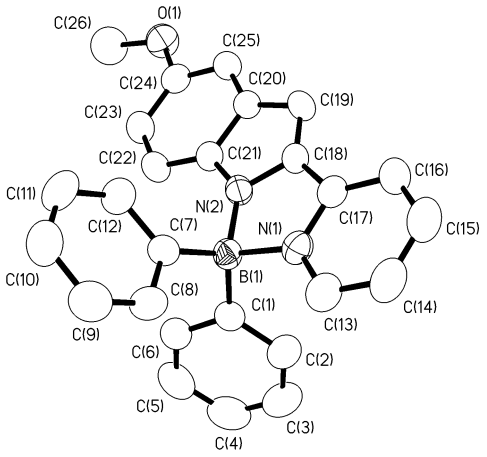

Figure 2. Molecular structure of **5c** with 50% thermal ellipsoids and labeling schemes.

are occupied by the two phenyl groups. The B(1)−N(2) indole bond (1.5538(15) Å) is shorter than the B(1)−N(1) pyridyl bond (1.6326(16) Å), which is consistent with the fact that the indole nitrogen is anionic and hence a better donor than the neutral pyridyl nitrogen. The B−C and C−F bond lengths in **5a** are also in the normal range. The structure of compound **5b** is almost the same as that of compound **5a** except that the unit cell volume of **5b** (3972.3(18) Å^3) is slightly larger than that of **5a** (3903.8(11) Å^3), which could be due to the relatively large chlorine atom and the longer C−Cl bond length (1.774(2) Å) in **5b**, as compared to the C−F bond length (1.3686(14) Å) in **5a**. Except for this difference, the B−N and B−C bond lengths and bond angles in compound **5b** are quite similar to the corresponding bond lengths and angles in compound **5a**. The structural parameters of **5a** and **5b** are also similar to those reported[5] previously for BPh_2(2-PI).

The structure of compound **5c** is similar to those of **5a** and **5b**, as shown in Figure 2. Although the B−N(2) indole bond length (1.568(2) Å) is still shorter than the B−N(1) pyridyl bond length (1.639(3) Å) in compound **5c**, it is somewhat longer than the corresponding B−N indole bond length in compounds **5a** and **5b**. In contrast, the B−N pyridyl bond length in **5c** is similar to the corresponding bond length in **5a** and **5b**, indicating that the electron-withdrawing or -donating character of the substituent at the 5-position of the indolyl group can affect the bond length of the B−N(2) indole bond but does not make a significant difference for the bond length of the B−N(1) pyridyl bond. Electron-withdrawing groups tend to make the bond shorter, and an electron-donating group tends to make the bond somewhat longer. Although the molecular structure of compound **5c** resembles those of **5a** and **5b**, they crystallize in two different space groups: **5a** and **5b** belong to the monoclinic space group $C2/c$, while **5c** belongs to the triclinic space group $P\bar{1}$, and both are different from that[5] of BPh_2(2-PI). This difference is clearly caused by the size of the substituent at the 5-position of the indole ligand. It was observed previously that the subtle difference between BPh_2(2-PI) and BPh_2(2-PazI) causes a dramatic difference in thermal properties and crystal packing of the two compounds.[5] The different space groups and different thermal behavior of **5a**−**c** and BPh_2(2-PI) demonstrate this fact again.

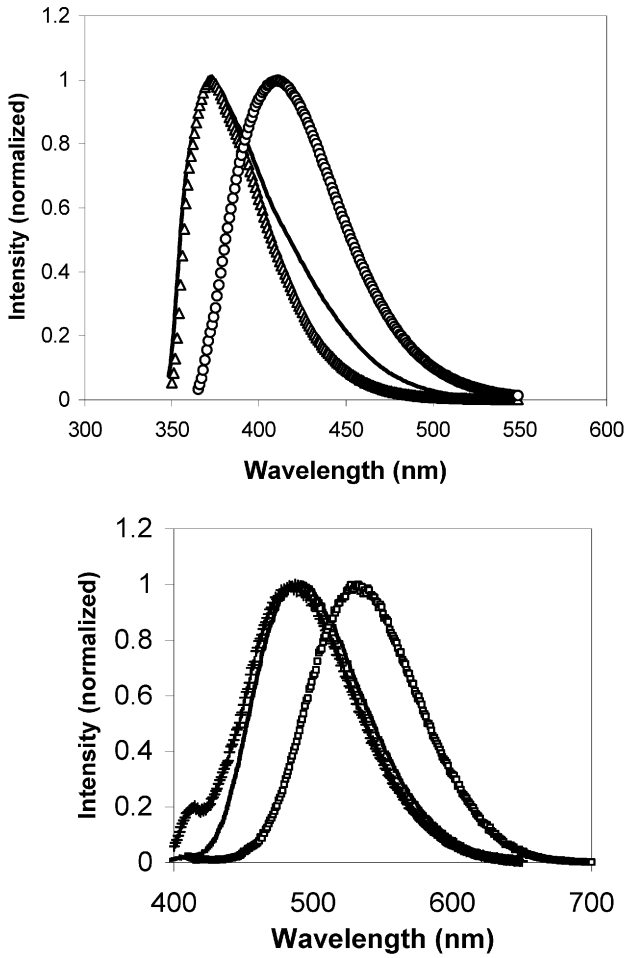

Figure 3. Top: Emission spectra of the free ligands **4a** (solid line), **4b** (empty triangles), and **4c** (empty circles). Bottom: Emission spectra of **5a** (solid line), **5b** (crosses), and **5c** (empty squares) in CH_2Cl_2 solution.

Photoluminescent (PL) and Electroluminescent (EL) Properties of Compounds 5a−c. Upon irradiation by UV light, compounds **5a−c** produce a bright blue/green color both in solution and in the solid state. As shown in Figure 3, the emission maximum of compounds **5a−c** in CH_2Cl_2 solution is at 490, 487, and 532 nm, respectively. These emissions are attributed to a $\pi^* \rightarrow \pi$ transition of the substituted 2-PI ligands, on the basis of previous ab initio molecular orbital calculations on BPh_2(2-PI) and BPh_2(2-PazI). The free ligands **4a−c** all display weak UV/blue emissions. The emission maximum of the free ligands **4a** and **4b** is very similar, $\lambda_{max} = 373$ nm. In contrast, the free ligand **4c** emits at $\lambda_{max} = 411$ nm. The red shift of the emission energy of the complexes as compared to that of the free ligands is due to the deprotonation of the free ligand, which causes a narrowing of the band gap. This observation is consistent with our previous studies on luminescent di(2-pyridyl)amine and 7-azaindole complexes, where the deprotonated ligands display a dramatic red shift in emission energy as compared to the neutral ligands due to narrowing of the $\pi^*-\pi$ gap.[11]

We have reported previously that BPh_2(2-PI) has a bright green luminescence at 516 nm both in solution and in the solid state. Compared with BPh_2(2-PI), the emission of complexes **5a**,**b**, with electron-withdrawing substituents, is blue-shifted by 25 nm to 490 nm, and the emission of complex **5c** with an electron-donating substituent is red-shifted by 16 nm to 532 nm. The free ligands display a similar trend of emission energy change. These results are consistent with our earlier ab initio molecular orbital calculations[5] on BPh_2(2-PI), which showed that the HOMO is a π-orbital with atomic orbital contributions almost exclusively from the indole moiety, while the LUMO is a π^*-orbital with atomic orbital contributions mostly from the pyridyl ring. Consequently, the electron-withdrawing fluorine or chlorine on the indole ring stabilizes or decreases the HOMO π-level,[13] hence increasing the LUMO(π^*)−HOMO(π) energy gap, while the electron-donating methoxy group destabilizes or increases the HOMO (π) energy level,[13] thus decreasing the LUMO(π^*)−HOMO(π) energy gap and resulting in a red shift of the emission energy. The ∼30 nm blue shift of the BPh_2(2-PazI) emission relative to BPh_2(2-PI), reported earlier by our group, is another example of the effect of an electronegative element (nitrogen) on the HOMO energy level.[5]

Fluorine is more electronegative than chlorine, and hence one would expect a greater blue shift of the emission energy for complex **5a** than for **5b**. The cause for the similar emission energies of **5a** and **5b** and the free ligands **4a** and **4b** is likely related to the interactions of the lone pair of the fluoro and chloro group with the π-orbitals of the indole ring, which can push the HOMO level up, hence decreasing the band gap. To confirm the involvement of lone-pair electrons, we performed ab initio molecular orbital calculations for compounds **5a** and **5b**. The geometric parameters from X-ray diffraction analysis were used for the calculation. The calculations were performed in a cc-pVDZ (correlation consistent double-ζ valence basis[14]) on an RHF (restricted Hartree−Fock) level of computation. The Gaussian suite of programs[15] was employed. The orbital diagrams were generated with the Molekel program.[16] All contour values are ±0.03 au. As shown in Figure 4, the HOMO, second HOMO, LUMO, and second LUMO are all π-type orbitals of the X-2-PI ligand and are very

(11) (a) Wu, Q.; Esteghamatian, M.; Hu, N.-X.; Popovic, Z. D.; Enright, G.; Breeze, S. R.; Wang, S. *Angew. Chem., Int. Ed.* **1999**, *38*, 985. (b) Hassan, A.; Wang, S. *J. Chem. Soc., Chem. Commun.* **1998**, 211. (c) Liu, W.; Hassan, A.; Wang, S. *Organometallics* **1997**, *16*, 4257. (d) Ashenhurst, J.; Brancaleon, L.; Hassan, A.; Liu, W.; Schmider, H.; Wang, S.; Wu, Q. *Organometallics* **1998**, *17*, 3186.

(12) (a) Drago, R. S. *Physical Methods in Chemistry*; W. B. Saunders Company: Philadelphia, 1977; Chapter 5. (b) Masetti, F.; Mazzucato, U.; Galiazzo, G. *J. Lumin.* **1971**, *4*, 8. (c) Werner, T. C.; Hawkins, W.; Facci, J.; Torrisi, R.; Trembath, T. *J. Phys. Chem.* **1978**, *82*, 298. (d) Bluemer, G. P.; Zander, M.; Ruetgerswerke, A. G. *Z. Naturforsch. A* **1979**, *34A*, 909.

(13) Carey, F. A.; Sundberg, R. J. *Advanced Organic Chemistry*, *Part A*: *Structure and Mechanisms*, 3rd ed.; Plenum Press: New York, 1990; Chapter 10.

(14) Wong, D. E.; Dunning, T. H., Jr. *J. Chem. Phys.* **1993**, *98*, 1358.

(15) Frisch, M. J.; Trucks, G. W.; Schlegel, H. B.; Scuseria, G. E.; Robb, M. A.; Cheeseman, J. R.; Zakrzewski, V. G.; Montgomery, J. A., Jr.; Stratmann, R. E.; Burant, J. C.; Dapprich, S.; Millam, J. M.; Daniels, A. D.; Kudin, K. N.; Strain, M. C.; Farkas, O.; Tomasi, J.; Barone, V.; Cossi, M.; Cammi, R.; Mennucci, B.; Pomelli, C.; Adamo, C.; Clifford, S.; Ochterski, J.; Petersson, G. A.; Ayala, P. Y.; Cui, Q.; Morokuma, K.; Malick, D. K.; Rabuck, A. D.; Raghavachari, K.; Foresman, J. B.; Cioslowski, J.; Ortiz, J. V.; Stefanov, B. B.; Liu, G.; Liashenko, A.; Piskorz, P.; Komaromi, I.; Gomperts, R.; Martin, R. L. D.; Fox, J.; Keith, T.; Al-Laham, M. A.; Peng, C. Y.; Nanayakkara, A.; Gonzalez, C.; Challacombe, M.; Gill, P. M. W.; Johnson, B.; Chen, W.; Wong, M. W.; Andres, J. L.; Gonzalez, C.; Head-Gordon, M.; Replogle, E. S.; Pople, J. A. *Gaussian 98*, revision A.6; Gaussian, Inc.: Pittsburgh, PA, 1998.

(16) Flkiger, P.; Lthi, H. P.; Portmann, S.; Weber, J. *MOLEKEL*, *4.1*; Swiss Center for Scientific Computing: Manno (Switzerland), 2000−2001.

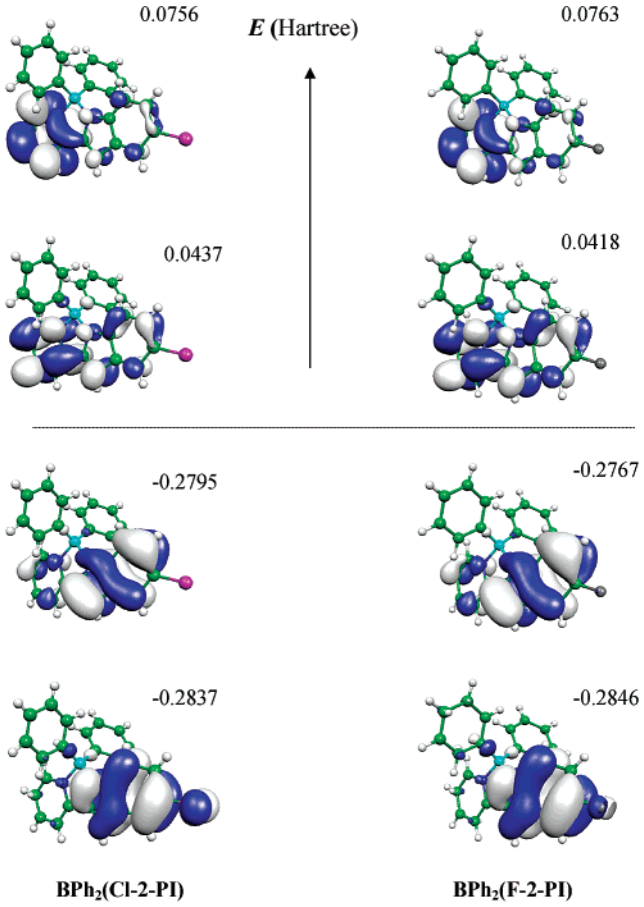

Figure 4. HOMO, second HOMO, LUMO, and second LUMO of compounds **5a** and **5b**.

similar for both compounds in terms of appearance and energy. The HOMO and second HOMO are near degenerate. Likewise, the LUMO and second LUMO are also near degenerate. The HOMO and second HOMO for both molecules consist of mostly atomic orbitals of the indolyl ring. The lone-pair orbital of the halogen atom has a significant contribution in the second HOMO. The LUMO and second LUMO consist of atomic orbitals from both pyridyl and indolyl rings with a dominant pyridyl contribution. Perhaps, because the lone-pair orbital of the fluorine atom can overlap relatively efficiently with the π-orbitals of the indole ring due to the compatible size and energy of 2p-orbitals from carbon and fluorine atoms, compared to that of the chlorine atom, the band gap increase due to the more electronegative nature of the fluorine atom is partially compensated, thus leading to the similar band gap for compounds **5a** and **5b**.

In the solid state, the emission of **5a** and **5b** is found at $\lambda = 503$ and 500 nm, respectively. This slight red shift may be caused by intermolecular interactions in the solid state. There is almost no shift of the solid state emission for complex **5c** and BPh_2(2-PI), which is found at 516 and 530 nm, respectively. Substituent effects on luminescence are well documented for a variety of compounds.[17] However, no systematic study on the luminescence of boron compounds has been reported.

(17) (a) Madej, S. L.; Okajima, S.; Lim, E. C. *J. Chem. Phys.* **1976**, *65*, 1219. (b) King, L. A. *J. Chem. Soc., Perkin Trans.* **1977**, *7*, 919. (c) Tine, A.; Aaron, J. J. *Can. J. Spectrosc.* **1984**, *29*, 121. (d) Hotchandani, S.; Testa, A. C. *J. Lumin.* **1994**, *59*, 59.

Table 3. Photoluminescence Data for Complexes 5a−c and BPh_2(2-PI)$_2$

complex	emission λ_{max} (nm) CH_2Cl_2, 298 K	emission λ_{max} (nm) solid, 298 K	excitation wavelength (nm)	quantum yields[a]
5a	490	503	376	0.33
5b	487	500	376	0.22
BPh_2(2-PI)$_2$	516	516	376	0.29
5c	532	530	396	0.036

[a] Relative to 9,10-diphenylanthracene in CH_2Cl_2 at 298 K.

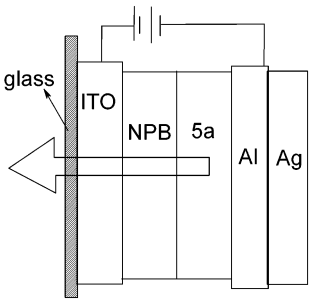

Figure 5. Diagram showing the EL device structure of **5a**.

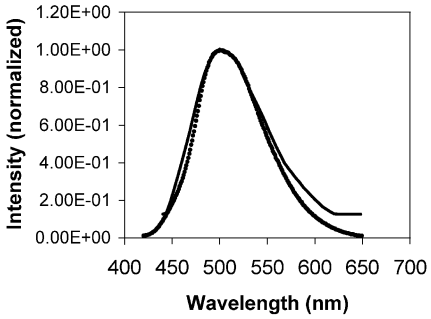

Figure 6. PL spectrum of **5a** (solid circles) and EL spectrum of the device (solid line).

Emission quantum yields were measured for compounds **5a−c** and BPh_2(2-PI). Among all the complexes, compound **5a** has the highest quantum yield (0.32), slightly higher than that of BPh_2(2-PI) (0.29). The quantum yield of compound **5b** (0.22) is lower than that of BPh_2(2-PI), which is due to the heavy-atom effect[12] of the chlorine substituent, which leads to a slight luminescence quenching. Compound **5c** has a low quantum yield (0.036), which is most likely due to the thermal motion of the conformationally mobile methoxy group, which results in energy loss via nonradiative decay. The photoluminescent properties of compounds **5a−c** and BPh_2(2-PI) are summarized in Table 3.

Compounds **5a** and **5b** are suitable candidates as emitters for EL devices because of their high emission efficiency, high melting points, high volatility, and good chemical stability. Since compound **5a** has the highest emission quantum yield, and its emission energy was blue-shifted to blue/green color in comparison with BPh_2(2-PI), an EL device was fabricated with compound **5a** as the emitting layer and the electron transport layer. The EL device (Figure 5) consists of two layers, a hole transport layer made of NPB and an emitting and electron transport layer made of compound **5a**. The EL device emits blue-green light with an emission maxi-

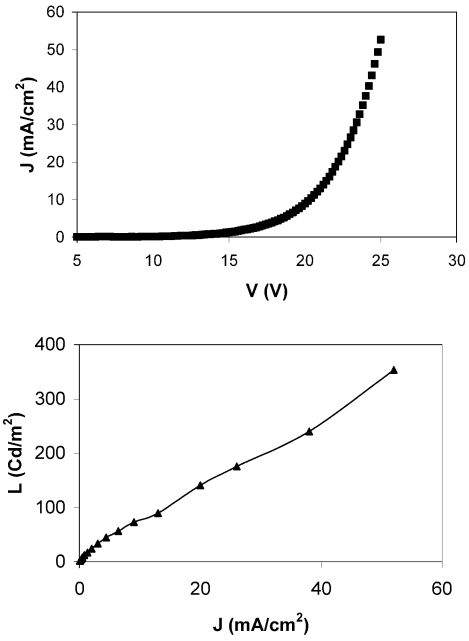

Figure 7. *J*−*V* (top) and *L*−*J* (bottom) plots of the EL device.

mum at 502 nm (Figure 6). The EL spectrum from the device matches very well the PL spectrum of **5a** in the solid state, indicating that the observed EL originates from compound **5a**. The *J*−*V* and *L*−*J* characteristics of the EL device are shown in Figure 7. The turn-on voltage of the device is 11 V. Although the turn-on voltage is relatively high in comparison to previously reported EL devices based on boron chelate compounds, due to the absence of an electron transport layer, it shows that compound **5a** is capable of functioning as an emitter and an electron transport material as well. The EL device is fairly bright, as shown by the luminance of 141 cd/m^2 at 20 mA/cm^2 and the external efficiency of 0.82 cd/A at 20 mA/cm^2.

In summary, three new blue/green luminescent boron complexes based on 5-substituted 2-PI ligands have been synthesized and characterized. These compounds demonstrate that the emission of 2-PI boron chelate complexes can be tuned by using appropriate substituent groups. An electron-withdrawing group such as fluoride and chloride causes a blue shift of the emission energy, while an electron-donating group such as methoxy causes a red shift. The fluoro-substituted compound **5a** appears to be the most promising as an emitter for EL displays due to its high emission efficiency and high melting point. Further substitution on the indole ring by additional fluorine atoms could drive the emission energy further into the blue region (∼450 nm), providing new stable blue emitters, and such efforts are being undertaken in our laboratory.

Acknowledgment. S.W. and Q.L. thank the Natural Sciences and Engineering Research Council of Canada, and R.T. and M.M. thank the NSF (CHE-9714998) and the Robert A. Welch Foundation (E-621) for financial support.

Supporting Information Available: X-ray diffraction data for **5a**−**c**, including tables of atomic coordinates, thermal parameters, bond lengths and angles, and hydrogen parameters. This material is available free of charge via the Internet at http://pubs.acs.org.

OM020446J